Supporting Information

Photoassisted photoluminescence fine-tuning of gold nanodots through free radical-mediated ligand-assembly

Yu-Ting Tseng,[‡a] Rochelle Cherng,[‡b] Scott G. Harroun,[c] Zhiqin Yuan,[d] Tai-Yuan Lin,[e] Chien-Wei Wu,[a] Huan-Tsung Chang,*[a] and Chih-Ching Huang*[bfg]

[a]Department of Chemistry, National Taiwan University, Taipei, 10617, Taiwan

[b]Department of Bioscience and Biotechnology, National Taiwan Ocean University, Keelung, 20224, Taiwan

[c]Department of Chemistry, Université de Montréal, Montreal, Quebec, Canada

[d]State Key Laboratory of Chemical Resource Engineering, Beijing University of Chemical Technology, Beijing, 100029, China

[e]Institute of Optoelectronic Sciences, National Taiwan Ocean University, Keelung, 20224, Taiwan

[f]Center of Excellence for the Oceans, National Taiwan Ocean University, Keelung, 20224, Taiwan

[g]School of Pharmacy, College of Pharmacy, Kaohsiung Medical University, Kaohsiung, 80708, Taiwan

[‡]These authors contributed equally.

Correspondence: Prof. Huan-Tsung Chang, Department of Chemistry, National Taiwan University, 1, Section 4, Roosevelt Road, Taipei 10617, Taiwan; tel. and fax: 011-886-2-3366-1171; e-mail: changht@ntu.edu.tw; Prof. Chih-Ching Huang, Department of Bioscience and Biotechnology, National Taiwan Ocean University, 2, Beining Road, Keelung 20224, Taiwan; tel.: 011-886-2-2462-2192 ext5517; fax: 011-886-2-2462-2320; e-mail: huanging@ntou.edu.tw

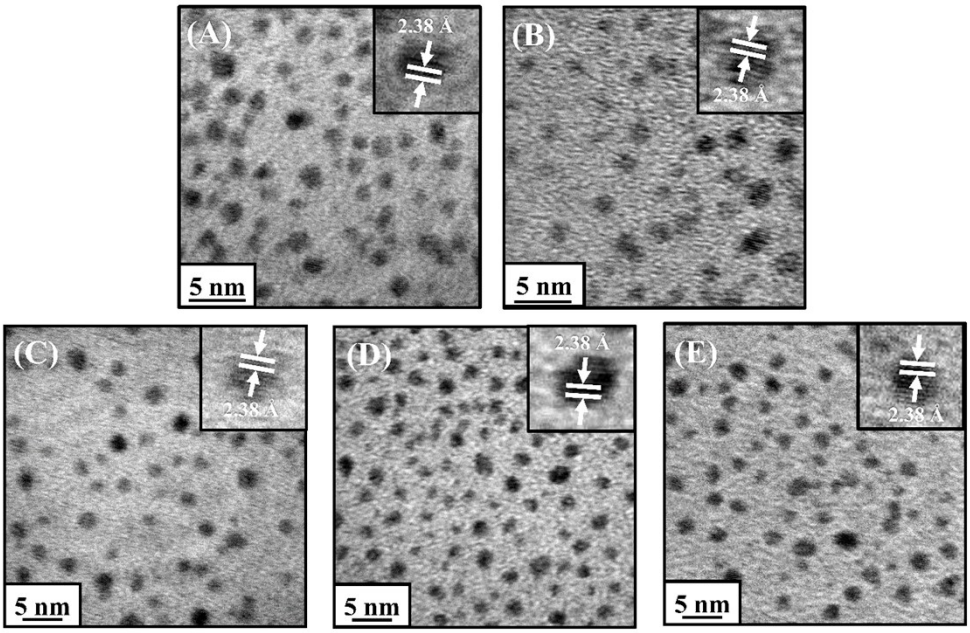

Figure S1. TEM images of (A) 11-MUTAB–Au NDs, (B) 11-MUA/11-MUTAB–Au $NDs_{UV\text{-}5}$, (C) 11-MUA/11-MUTAB–Au $NDs_{UV\text{-}15}$, (D) 11-MUA/11-MUTAB–Au $NDs_{UV\text{-}30}$, and (E) 11-MUA/11-MUTAB–Au $NDs_{UV\text{-}60}$. Insets: High-resolution TEM images.

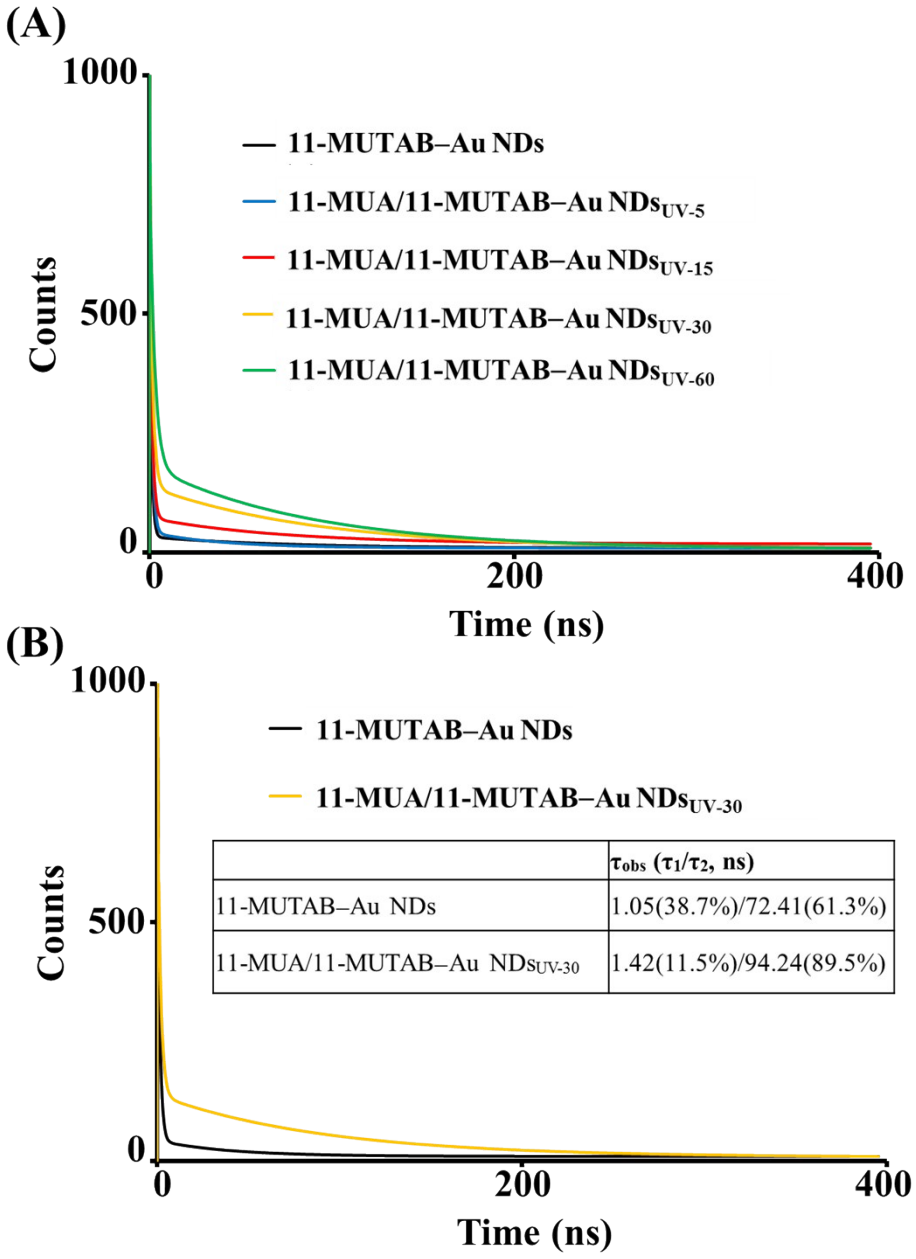

	τ_{obs} (τ_1/τ_2, ns)
11-MUTAB–Au NDs	1.05(38.7%)/72.41(61.3%)
11-MUA/11-MUTAB–Au NDs_{UV-30}	1.42(11.5%)/94.24(89.5%)

Figure S2. (A) PL lifetimes of as-prepared 11-MUTAB–Au NDs, 11-MUA/11-MUTAB–Au NDs_{UV-5}, 11-MUA/11-MUTAB–Au NDs_{UV-15}, 11-MUA/11-MUTAB–Au NDs_{UV-30}, and 11-MUA/11-MUTAB–Au NDs_{UV-60} excited with a pulsed laser at 375 nm. (B) PL lifetimes of as-prepared 11-MUTAB–Au NDs and 11-MUA/11-MUTAB–Au NDs_{UV-30} excited with a pulsed laser at 390 nm. The PL decay was fitted to a biexponential decay. The fitted lifetimes for (A) were listed in Table 1. Other conditions were the same as those described in Figure 1.

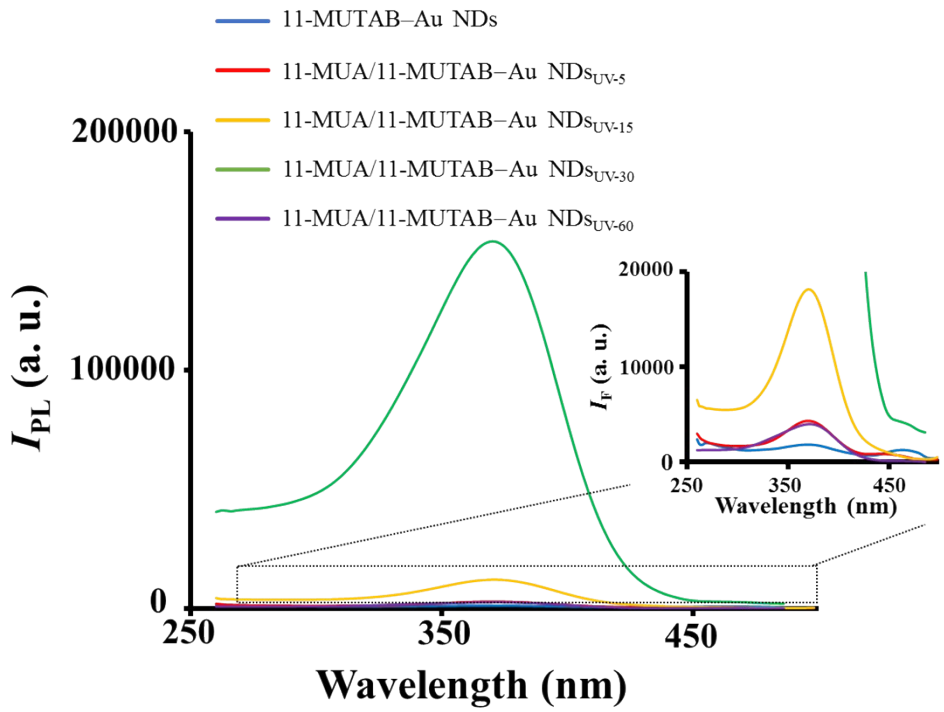

Figure S3. PL excitation spectra of 11-MUTAB–Au NDs, 11-MUA/11-MUTAB–Au NDs$_{UV-5}$, 11-MUA/11-MUTAB–Au NDs$_{UV-15}$, 11-MUA/11-MUTAB–Au NDs$_{UV-30}$, and 11-MUA/11-MUTAB–Au NDs$_{UV-60}$. The solutions of as-prepared Au NDs were diluted 10-fold in 20 mM sodium tetraborate solution (pH 9.2). The PL intensities (I_{PL}) are plotted in arbitrary units (a. u.). The emission wavelength was set at λ_{max}^{em} for each Au NDs (Table 1). Other conditions were the same as those described in Figure 1.

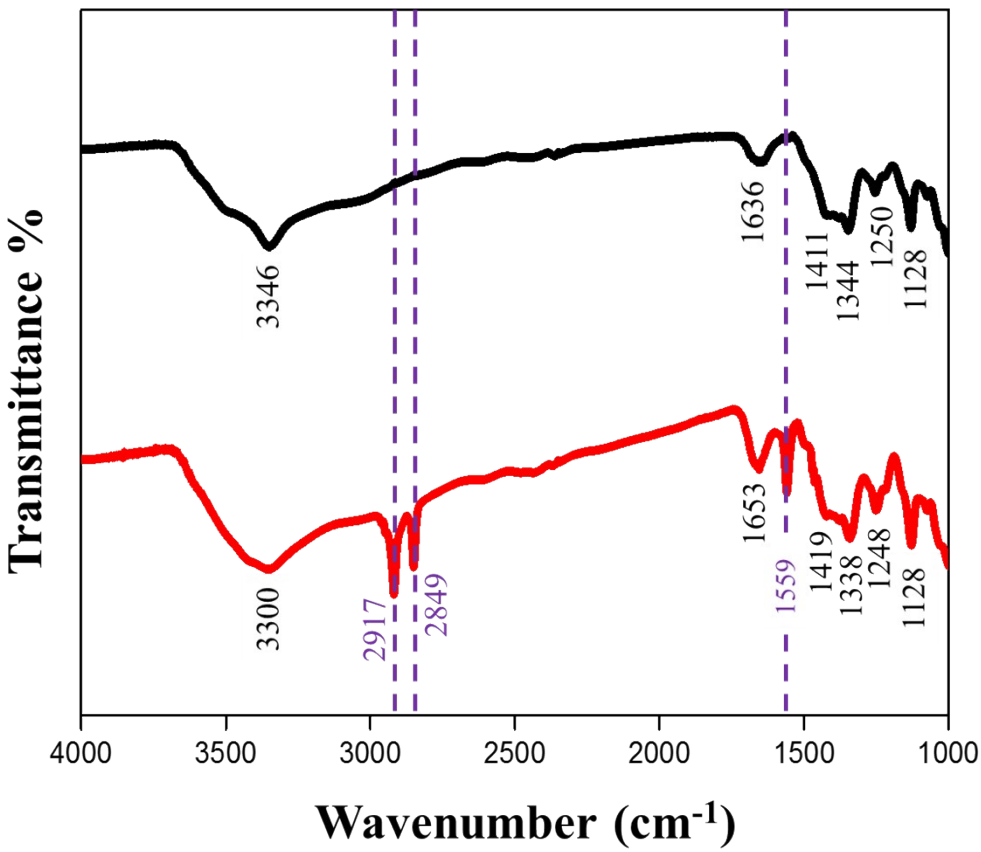

Figure S4. FT-IR spectra of as-prepared 11-MUTAB–Au NDs (black) and 11-MUA/11-MUTAB–Au $NDs_{UV\text{-}30}$ (red). The IR absorption bands at ~1128, ~1250, ~1340, ~1415, ~1560, ~1640, ~2900, and ~3300 cm^{-1} are assigned to C–H wag, C–N stretch, C–H rock, C–H bend, C=O stretch band (carboxylate salts), N–H bend, O–H stretch band (carboxylic acid), and O–H stretch vibrational modes, respectively. Compared to the 11-MUTAB–Au NDs, 11-MUA/11-MUTAB–Au $NDs_{UV\text{-}30}$ exhibited C=O stretch band (carboxylate salts) (1559 cm^{-1}) and O–H stretch band (carboxylic acid) (~2900 cm^{-1}), further confirming the conjugation of 11-MUA units on the surfaces of the latter species.

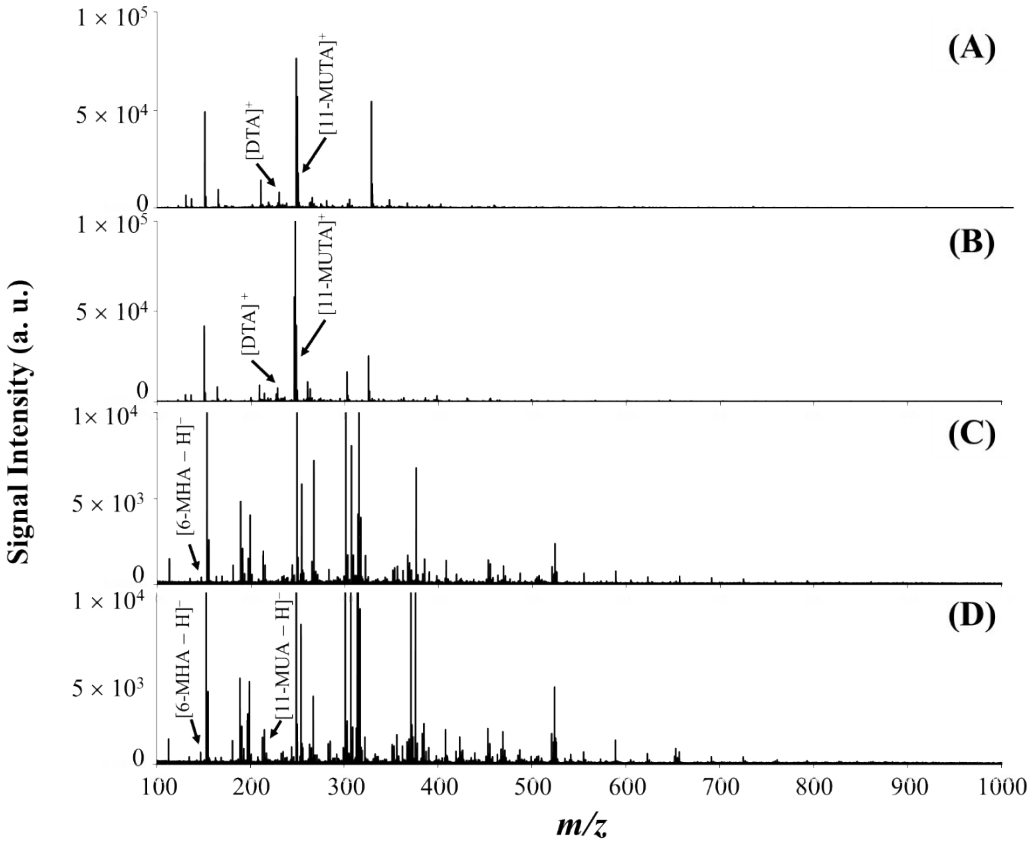

Figure S5. ESI-Q-TOF MS mass spectra of (A) and (C) purified 11-MUTAB–Au NDs and (B) and (D) purified 11-MUA/11-MUTAB–Au $NDs_{UV\text{-}30}$ recorded in (A) and (B) positive and (C) and (D) negative MS modes. Signals at *m*/*z* 228.26, 246.73, 147.04, and 217.12 are assigned to [dodecyltrimethylammonium]$^+$ ([DTA]$^+$), [(11-mercaptoundecyl)-*N*,*N*,*N*-trimethylammonium]$^+$ ([11-MUTA]$^+$), [6-mercaptohexanoic acid – H]$^-$ ([6-MHA – H]$^-$), and [11-mercaptoundecanoic acid – H]$^-$ ([11-MUA – H]$^-$) ions, respectively. The dodecyltrimethylammonium chloride (DTAC) and 6-mercaptohexanoic acid (6-MHA) are used as internal standards in negative and positive MS modes, respectively. The MS signal intensities are plotted in arbitrary units (a. u.). Other conditions were the same as those described in Figure 1. The concentration of 11-MUTAB and 11-MUA ligands in purified Au ND solutions listed in Table 1 were determined by measuring the relative MS signals of [11-MUTA]$^+$/[DTA]$^+$ and [11-MUA – H]$^-$/[6-MHA – H]$^-$ in the samples and comparing to the calibration curve with internal standards, respectively.

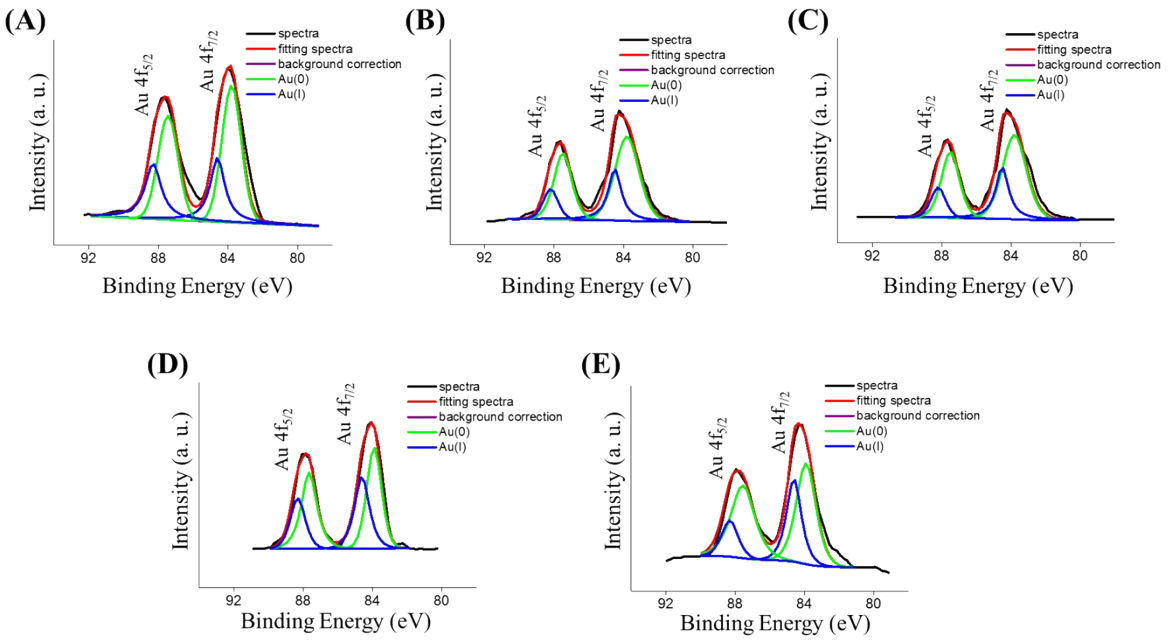

Figure S6. XPS spectra of (A) 11-MUTAB–Au NDs, (B) 11-MUA/11-MUTAB–Au $NDs_{UV\text{-}5}$, (C) 11-MUA/11-MUTAB–Au $NDs_{UV\text{-}15}$, (D) 11-MUA/11-MUTAB–Au $NDs_{UV\text{-}30}$, and (E) 11-MUA/11-MUTAB–Au $NDs_{UV\text{-}60}$. The broad peaks (Au $4f_{7/2}$ and Au $4f_{5/2}$) were deconvoluted into two distinct components (green and blue lines) centered at binding energies of 83.9/84.6 eV and 87.5/88.3 eV for assigning to Au(0)/Au(I) species, respectively. Other conditions were the same as those described in Figure 1.

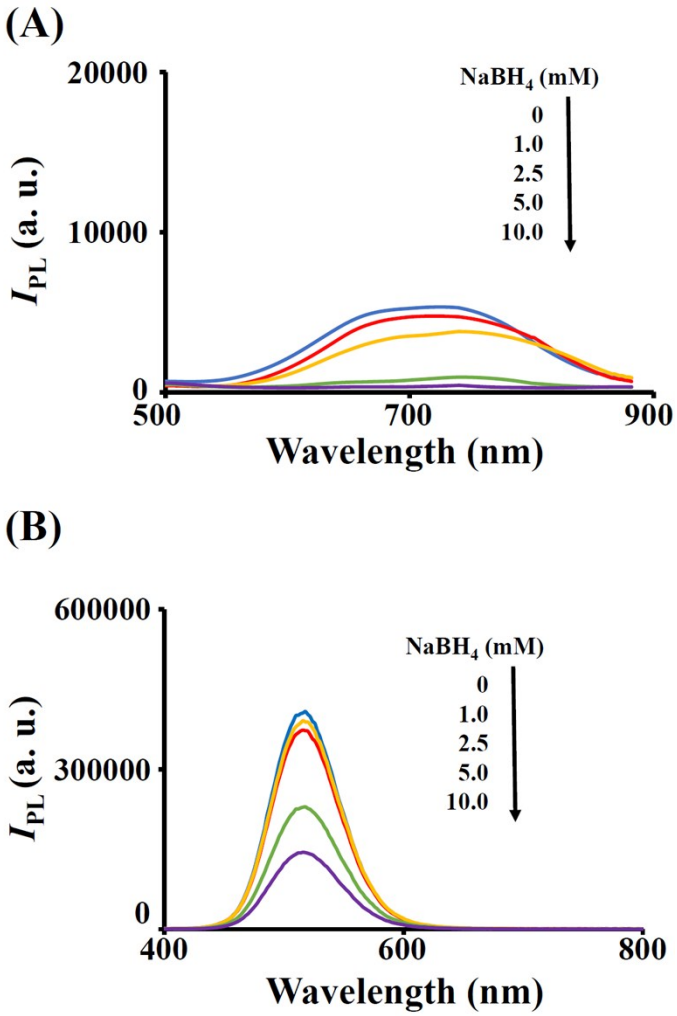

Figure S7. PL spectra of (A) 11-MUTAB–Au NDs (100 nM) and (B) 11-MUA/11-MUTAB–Au $NDs_{UV\text{-}30}$ (100 nM) after treatment with 0–10.0 mM $NaBH_4$ in 5 mM sodium phosphate buffer (pH 7.0) for 2 h. Other conditions were the same as those described in Figure 1.

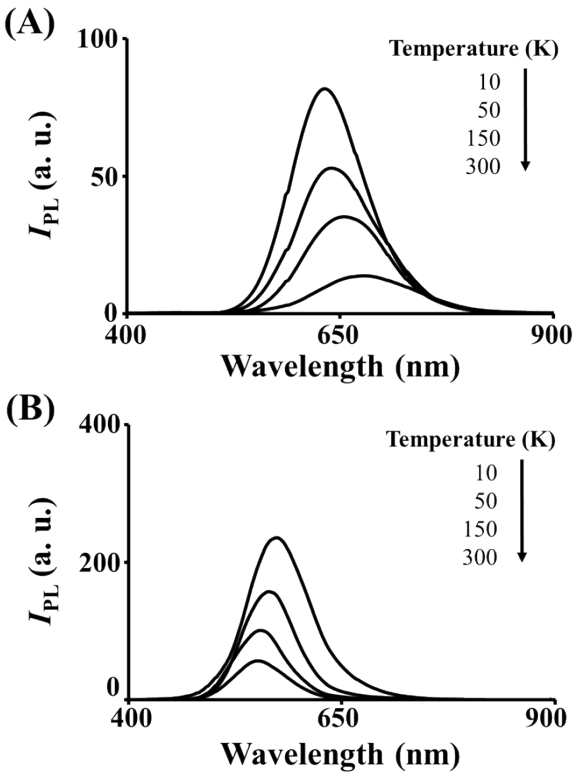

Figure S8. Temperature-dependent (10–300 K) PL emission spectra of (A) 11-MUTAB–Au NDs and (B) 11-MUA/11-MUTAB–Au $NDs_{UV\text{-}30}$ in sodium tetraborate solution (20 mM, pH 9.2). Other conditions were the same as those described in Figure 1.

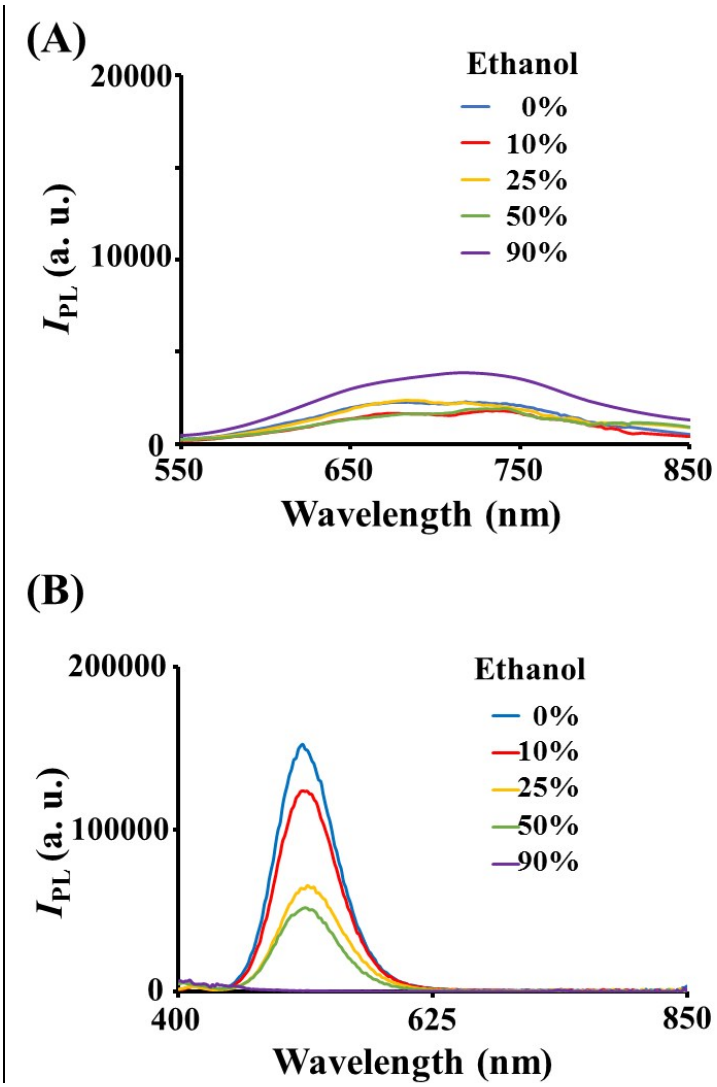

Figure S9. PL spectra of (A) 11-MUTAB–Au NDs (100 nM) and (B) 11-MUA/11-MUTAB–Au $NDs_{UV\text{-}30}$ (100 nM) in sodium tetraborate solution (20 mM, pH 9.2) containing ethanol (0−90%). Other conditions were the same as those described in Figure 1.

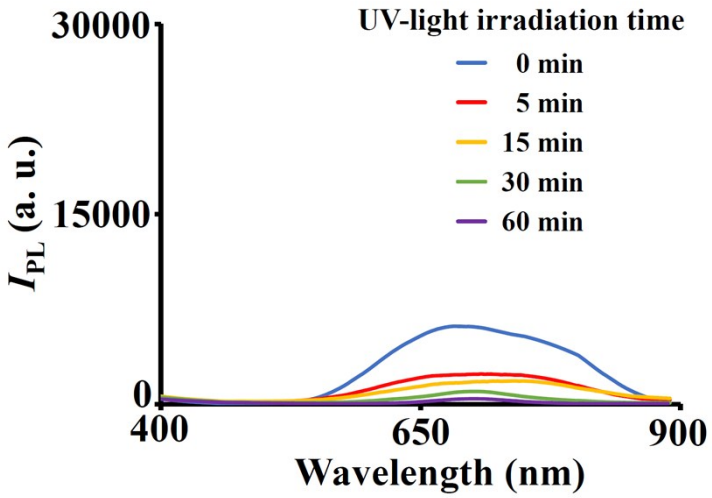

Figure S10. PL spectra of 11-MUTAB–Au NDs in the absence of 11-MUA under UV-light irradiation for 5−60 min. Other conditions were the same as those described in Figure 1.

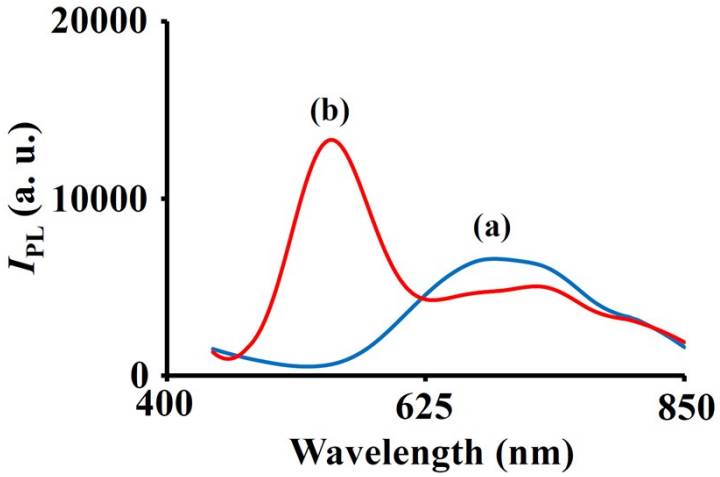

Figure S11. PL spectra of 11-MUTAB–Au NDs (500 nM) reacted with 11-MUA (5 mM) in sodium tetraborate solution (20 mM, pH 9.2) in the dark for (a) 0 h and (b) 48 h. Other conditions were the same as those described in Figure 1.

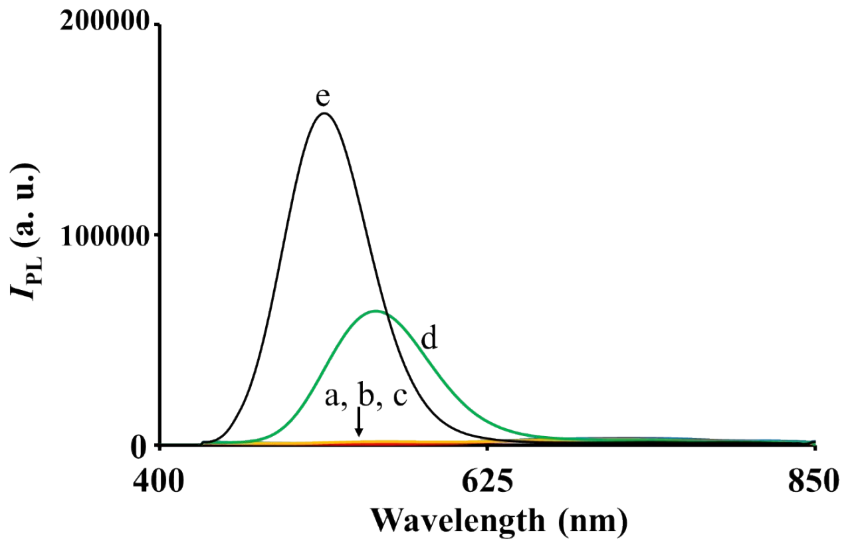

Figure S12. PL spectra of (a–d) 11-MUA–Au NDs synthesized for (a) 6 h, (b) 1 day, (c) 2 days, (d) 5 days, and (e) 11-MUA/11-MUTAB–Au $NDs_{UV\text{-}30}$. The solutions of as-synthesized Au NDs were diluted 10-fold in 20 mM sodium tetraborate solution (pH 9.2). Other conditions were the same as those described in Figure 1.

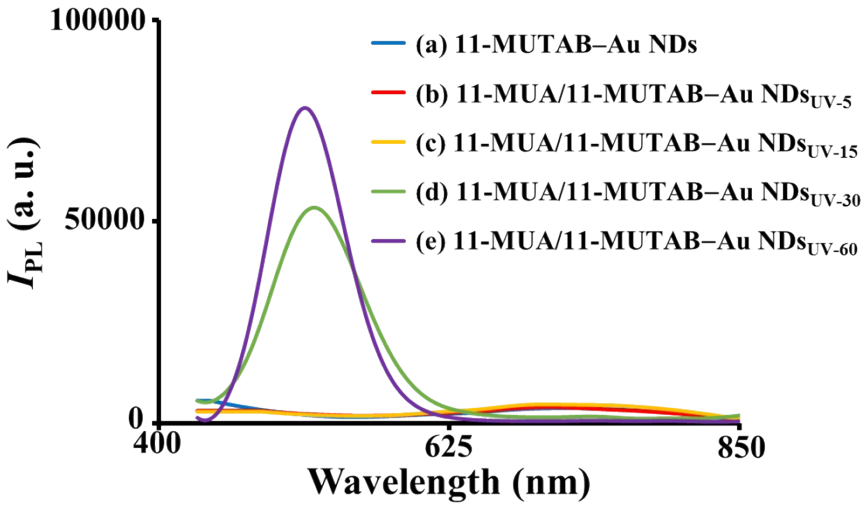

Figure S13. PL spectra of (a) 11-MUTAB–Au NDs, (b) 11-MUA/11-MUTAB–Au NDs_{UV-5}, (c) 11-MUA/11-MUTAB–Au NDs_{UV-15}, (d) 11-MUA/11-MUTAB–Au NDs_{UV-30}, and (e) 11-MUA/11-MUTAB–Au NDs_{UV-60} prepared under N_2 atmosphere. Other conditions were the same as those described in Figure 1.

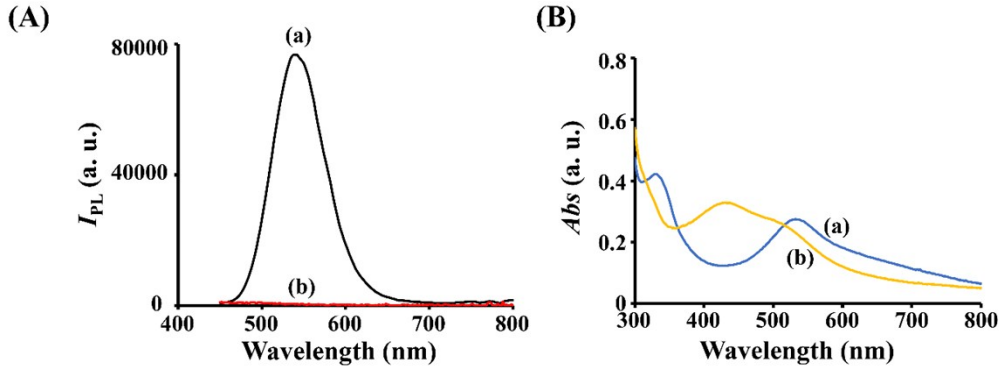

Figure S14. (A) PL spectra of 11-MUA/11-MUTAB−Au NDs_{UV-30} solutions prepared in the (a) absence and (b) presence of 1,1-diphenyl-2-picryl-hydrazyl (DPPH; 50 μM). (B) UV-Vis absorption spectra of DPPH (50 μM) before (a) and after (b) reaction with 11-MUA/11-MUTAB−Au NDs under UV-light irradiation for 30 min.

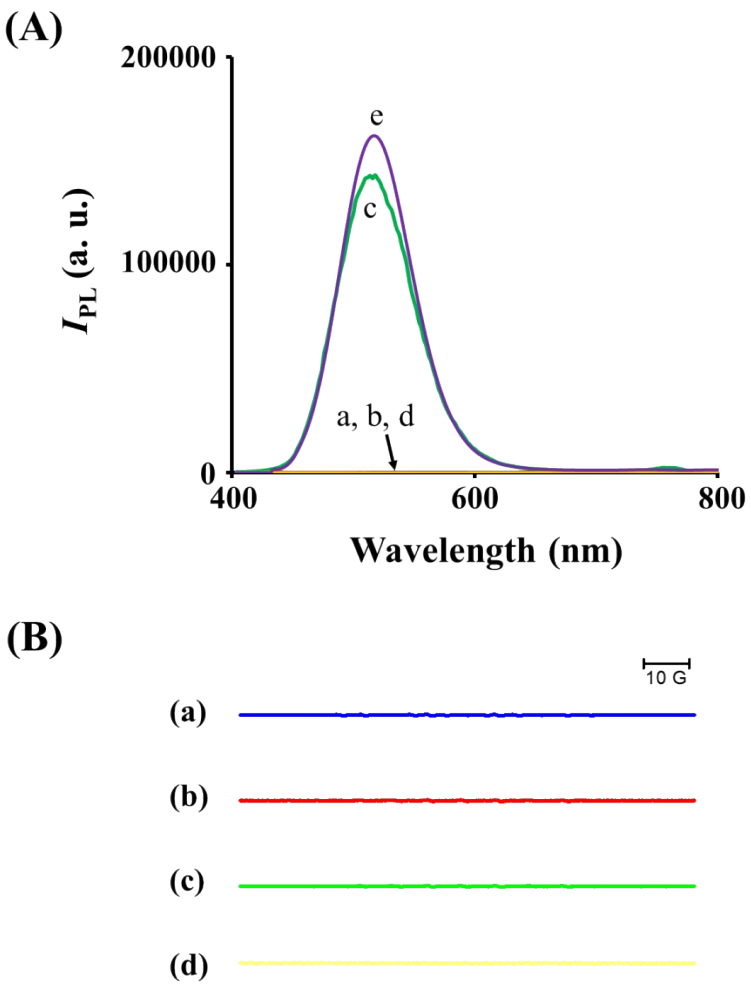

Figure S15. PL spectra of (a–d) 11-MUA/11-MUTAB–Au NDs synthesized in the dark at (a) 20 °C, (b) 40 °C, (c) 60 °C, (d) 80 °C, and (e) 11-MUA/11-MUTAB–Au $NDs_{UV\text{-}30}$. (B) ESR spectra of the 5,5-dimethyl-1-pyrroline N-oxide (DMPO, 100 mM) adducts in solutions of (a–d) 11-MUA/11-MUTAB–Au NDs synthesized in the dark at (a) 20 °C, (b) 40 °C, (c) 60 °C, and (d) 80 °C. The solutions of as-prepared Au NDs were diluted 10-fold in 20 mM sodium tetraborate solution (pH 9.2). Other conditions were the same as those described in Figure 1.

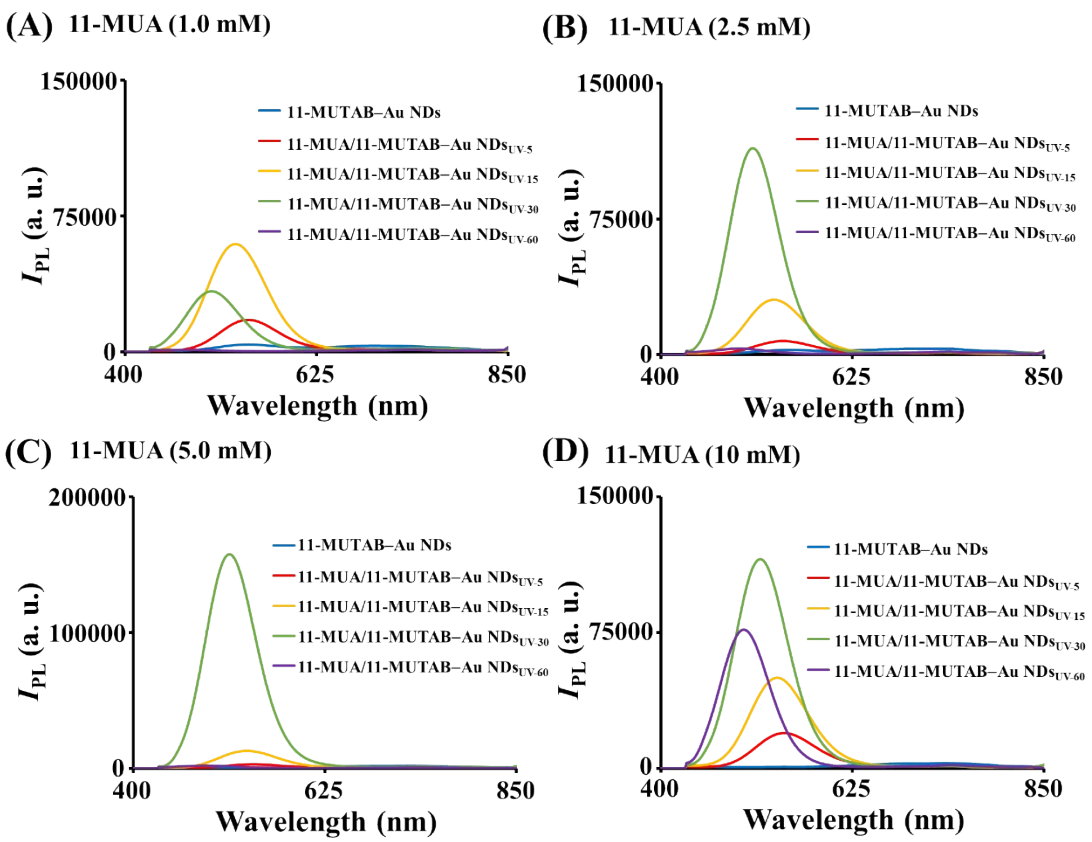

Figure S16. PL spectra of 11-MUTAB–Au NDs, 11-MUA/11-MUTAB–Au NDs$_{UV-5}$, 11-MUA/11-MUTAB–Au NDs$_{UV-15}$, 11-MUA/11-MUTAB–Au NDs$_{UV-30}$, and 11-MUA/11-MUTAB–Au NDs$_{UV-60}$ using (A) 11-MUA (1.0 mM), (B) 11-MUA (2.5 mM), (C) 11-MUA (5.0 mM) and (D) 11-MUA (10 mM) for assembly of the 11-MUTAB–Au NDs under UV-light irradiation. Other conditions were the same as those described in Figure 1.

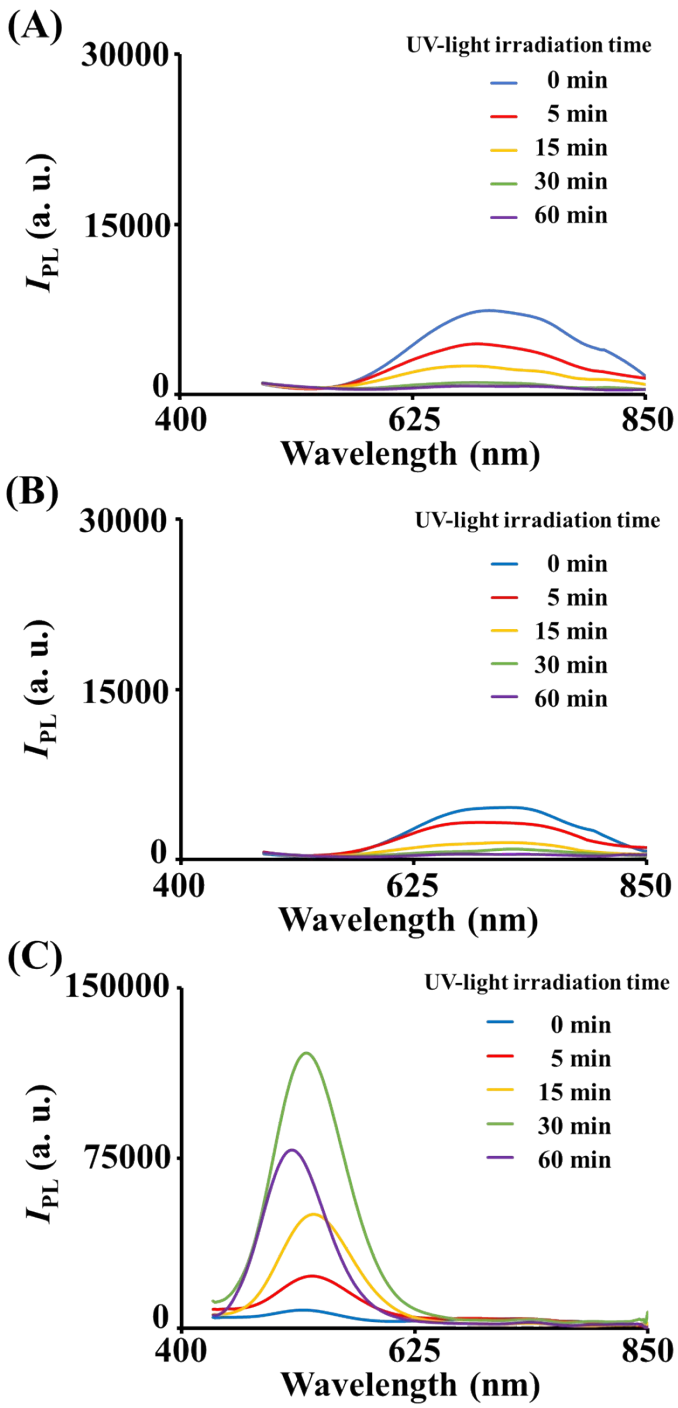

Figure S17. PL spectra of 11-MUTAB–Au NDs after assembly with (A) 3-MPA (5 mM), (B) 6-MHA (5 mM), and (C) 16-MHDA (5 mM) under UV-light irradiation (0–60 min). Other conditions were the same as those described in Figure 1.

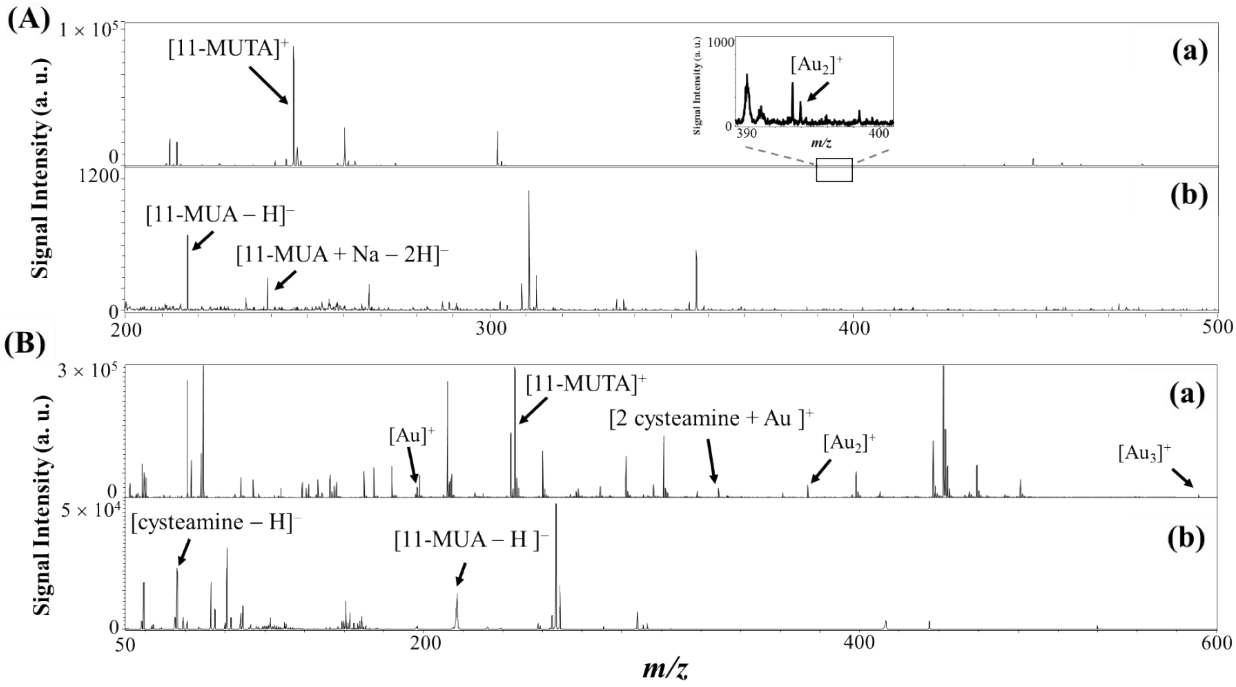

Figure S18. LDI-MS spectra of (A) purified 11-MUA/11-MUTAB–Au $NDs_{UV\text{-}30}$ in sodium tetraborate solution (20 mM, pH 9.2) and (B) 11-MUA/11-MUTAB–Au $NDs_{UV\text{-}30}$ after treated with cysteamine (10 mM) for 5 min under UV-light irradiation and then purification. The LDI-MS were recorded in (a) and (b) are positive and negative modes, respectively. Signals at *m*/*z* 246.73, 393.83, 217.12 and 238.09 in (A) are assigned to $[11\text{-MUTA}]^+$, $[Au_2]^+$, $[11\text{-MUA} - H]^-$ and $[11\text{-MUA} + Na - 2H]^-$ ions, respectively. Signals at *m*/*z* 196.96, 246.73, 351.02, 393.83, 590.88, 77.03 and 217.12 in (B) are assigned to $[Au_1]^+$, $[11\text{-MUTA}]^+$, [2 cysteamine + Au]$^+$, $[Au_2]^+$, $[Au_3]^+$, $[\text{cysteamine} - H]^-$ and $[11\text{-MUA} - H]^-$ ions, respectively. A total of 1000 pulsed laser shots were applied to accumulate the signals from five LDI target positions under a laser power density of 6.37×10^4 W cm^{-2}. Signal intensities are plotted in arbitrary units (a. u.). Other conditions were the same as those described in Figure 3.

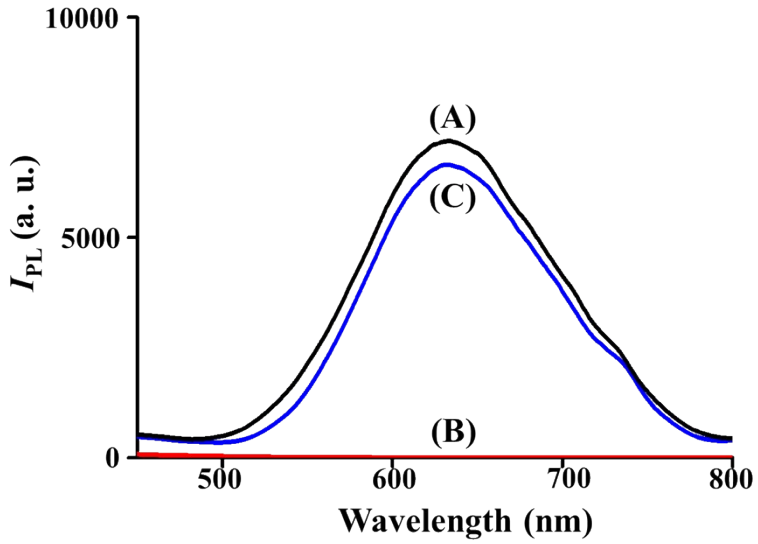

Fig. S19. PL emission spectra of (A) cysteamine/11-MUA/11-MUTAB–Au $NDs_{UV\text{-}30}$ (100 nM), (B) discarded solution after purification by centrifugal filtration (RCF 10,000 g; cutoff 10 kDa), and (C) resuspended cysteamine/11-MUA/11-MUTAB–Au $NDs_{UV\text{-}30}$ in 20 mM sodium tetraborate solution (pH 9.2). Other conditions were the same as those described in Figure 1.